



Improved charge density and stability in PDMS ferroelectrets using PDMS/PTFE composite materials

M. Zhang, J. Shi, S.P. Beeby^{*}

Centre for Flexible Electronics and E-Textiles, School of Electronics and Computer Science, University of Southampton, Southampton, UK

ARTICLE INFO

Keywords:

Ferroelectret
PDMS
PTFE
PDMS/PTFE composite coating

ABSTRACT

A ferroelectret is a flexible cellular polymer structure that generates electrical power under mechanical force. It behaves like a piezoelectric material in that a voltage is generated when the ferroelectret deforms. Its electrical output significantly depends on the surface charge density of the material used. Previous ferroelectrets fabricated from polydimethylsiloxane (PDMS) benefit from the soft, stretchable mechanical properties of the PDMS but the ability of this material to trap charge at its surface is poor. This paper presents approaches to enhance the surface charge density and stability of a PDMS based ferroelectret device by adding Polytetrafluoroethylene (PTFE) to the PDMS. This PDMS/PTFE composite has been evaluated when used to fabricate the ferroelectret device and when used as an additional coating the internal void surfaces of an otherwise plain PDMS ferroelectret. As the proportion of PTFE increases, the surface charge density on the void surfaces increases resulting in a corresponding increase in the piezoelectric properties of the ferroelectret. A weight ratio of PTFE powder and PDMS of 1:3 was found to achieve improved piezoelectric performance with an initial effective piezoelectric coefficient, d_{33e} , of around 700 pC/N which decayed initially and reached a steady state value of around 365 pC/N measured after 4 months after poling. This presents a considerable improvement in performance when compared with the effective d_{33e} of pure PDMS which has an initial value of around 110 pC/N and drops to below 8 pC/N after 4 months. The energy harvester potential of the ferroelectret was explored by cyclically compressing the PDMS/PTFE composite layer ferroelectret structure with a force of 500 N applied at 1 Hz. The output of the ferroelectret was found to charge a 10 μ F capacitor to 0.12 V after 40 s. Maximum output power occurs at a load resistance of 15 M Ω , with a peak power of 4 μ W. A fabricated PDMS/PTFE composite layer ferroelectret sample (weight ratio of PTFE powder and PDMS of 1:3) was also tested as a pressure sensor range from 0 to 500 N and achieved a sensitivity of 9.9 mV/N. The nonlinearity error of the proposed sensor was 1.7%.

1. Introduction

Energy harvesting refers to the conversion of energy from the surroundings into electrical energy. The available input energies typically include heat, light and mechanical vibrations/movements. Energy harvesting power supplies remove the need for a wired external power connection whilst also avoiding the use of a battery, resulting in maintenance free wireless device operation. Ferroelectrets are a form of smart material that has been considered for harvesting mechanical motion [1, 2].

Electrets are a type of dielectric material with the ability to semi-permanently trap charge trapped on the surface or in the bulk of the material and can be used to generate internal and external electric fields within devices. Ferroelectrets (also known as piezoelectrets) are

typically fabricated from electrets and contain voids that exploit the trapped charge and resulting electric fields to exhibit piezoelectric properties. Ferroelectrets were originally demonstrated as a thin film of polymer electret foam where the charge stored at the internal void surfaces produces an electric field across each void [3]. When compressed, the void height changes altering the dipole moments and producing compensating charges on the external surface of the foam as illustrated schematically in Fig. 1(a) [4,5]. The macroscopic behaviour of the ferroelectret is essentially the same as a piezoelectric material although the internal charge-generating mechanism is very different. Because of the low stiffness of the polymer electret materials and the presence of cavities and voids within the material, ferroelectrets are typically soft materials, compliant in the thickness direction resulting in improved piezoelectric properties compared with traditional

^{*} Correspondence to: School of Electronics and Computer Science, University of Southampton, Southampton, UK.

E-mail address: spb@ecs.soton.ac.uk (S.P. Beeby).

piezoelectric materials [6,7]. For example, effective piezoelectric coefficient d_{33e} values as high as 4050 pC/N have been achieved in Fluorinated ethylene propylene (FEP) ferroelectret polymer [8], compared with a standard effective piezoelectric coefficient d_{33e} of 17 pC/N for a polyvinylidene difluoride (PVDF) ferroelectric polymer [9] and 593 pC/N for a lead zirconate titanate (PZT) ferroelectric ceramic [10]. PZT ceramics are brittle (low fracture toughness) and have a high stiffness compared to the polymer ferroelectret materials [10]. Due to these outstanding piezoelectric and material properties, ferroelectrets have been used as functional materials in a variety of electromechanical sensor and actuator applications including human-machine interfaces [11,12].

Polydimethylsiloxane (PDMS) has been demonstrated in the fabrication of ferroelectrets with controlled void layouts and geometries rather than the random voids associated with foams [4]. Its primary advantages include low cost, fast simple fabrication and high levels of flexibility with a Young's modulus that can vary from 0.57 MPa to 3.7 MPa depending upon the degree of cross-linking [13]. Previous work at Southampton has developed a fabrication process for PDMS ferroelectrets with novel microscale void geometries [14]. However, PDMS is not a stable electret material and the surface charge stability on the void surfaces of the PDMS is poor, causing the effective piezoelectric coefficient of most samples to fall below 10 pC/N from around 110 pC/N in one month [15].

In contrast, Polytetrafluoroethylene (PTFE) exhibits excellent charge stability over time [16]. However, PTFE is not as soft or flexible as PDMS and is difficult to mold and shape mechanically. PTFE is typically processed as a powder rather than as a standard plastic, often using compression molding techniques or with the powder mixed with dispersants and applied as a coating by film casting [17,18]. The effect of adding PTFE particles to PDMS had been described in previous studies [19]. PTFE is a fluorocarbon and, since fluorine is the most electronegative element, PTFE will accept more electrons than PDMS [20]. Therefore, more electrons can be trapped on the surface of the PTFE particles, and as the ratio of PTFE particles within the PDMS increases, the surface charge density of the PDMS/PTFE composite will also increase [20].

This paper explores measures to combine PTFE in the form of a powder with the PDMS to improve the charge stability in the ferroelectret whilst retaining the compliant, flexible mechanical properties of the PDMS. This work explores two approaches for coating the surfaces of PDMS voids with a PTFE layer and an approach whereby the PTFE is added to the PDMS and the entire ferroelectret device is molded from the combined PDMS/PTFE material. A PTFE/water solution and PDMS/PTFE composite solution have been used to coat the void surfaces and the same PDMS/PTFE composite was used fabricate the whole ferroelectret.

2. Charge decay estimation

The charge stability in electrets is of great importance for the long-term application of electret and ferroelectret materials. For some electrets, it is very difficult to directly measure the life of electrets under normal temperature and humidity conditions within a reasonable time span. However, by using the isothermal depolarization procedure, experimental results obtained by increasing temperature to accelerate the attenuation of the electret's stored charge combined with suitable data processing, it is possible to describe the rate of charge decay. The electret charge decay has an approximately exponential relationship with time and temperature as given by Eq. 1 [18]:

$$\ln\tau(T) = \frac{E}{k} \times \frac{1}{T} + \ln\tau_0 \quad (1)$$

The parameter $\tau(T)$ in Eq. (1) represents the charge decay time constant at temperature T , where k is Boltzmann's constant and E , τ_0 is a constant. In the selected temperature range from 200 °C to 300 °C, by adjusting the ageing time, the equivalent surface charge density can be attenuated to a certain value, and the change over time under isothermal conditions can be measured. From this measured data, the effective time constant at each set depolarization temperature can be determined by Eq. (1). From (1), $\ln\tau$ and $1/T$ show a linear relationship and E , k , $\ln\tau_0$ can be considered as constants. Since the charge decay time constant of electrets at high temperatures are relatively short [18], this can be obtained by experimental measurements and the charge decay time constant at room temperature can be extrapolated from these results.

The linear relationship between charge decay and temperature for the ferroelectret materials with ratios of PTFE and PDMS varying from 1:10–1:2, the PTFE/water solution ferroelectret and the pure PDMS ferroelectret are shown in Fig. 1(b). These ratios were selected to enable the exploration of the effect of increasing the PTFE content on charge stability and on the physical properties of the PDMS. It is anticipated that the more PTFE added, the greater the charge stability but this will reduce physical properties such as the maximum strain the composite can survive. The maximum ratio of PTFE to PDMS was 1:2 which was limited by the viscosity of the formulation and the ability to mix it and evenly disperse the PTFE particles within the PDMS. The charge decay time constants for the electret at 200 °C, 250 °C and 300 °C were experimentally determined by isothermal depolarization. By extrapolating the plot to room temperature (25 °C, corresponding to $1/T$ equalling 0.00335 in Fig. 1(b)) the storage life of the surface charge at room temperature can be obtained where the charge storage life is defined as the time taken for the surface charge density to fall to 20%. The storage life at room temperature of the ferroelectret materials with ratios of PTFE and PDMS varying from 1:10–1:2 ranges from 270 years to 1097 years respectively (corresponding to $\ln\tau$ values of 5.6 and 7 in Fig. 1(b)). The charge storage life of the ferroelectret with the PTFE/

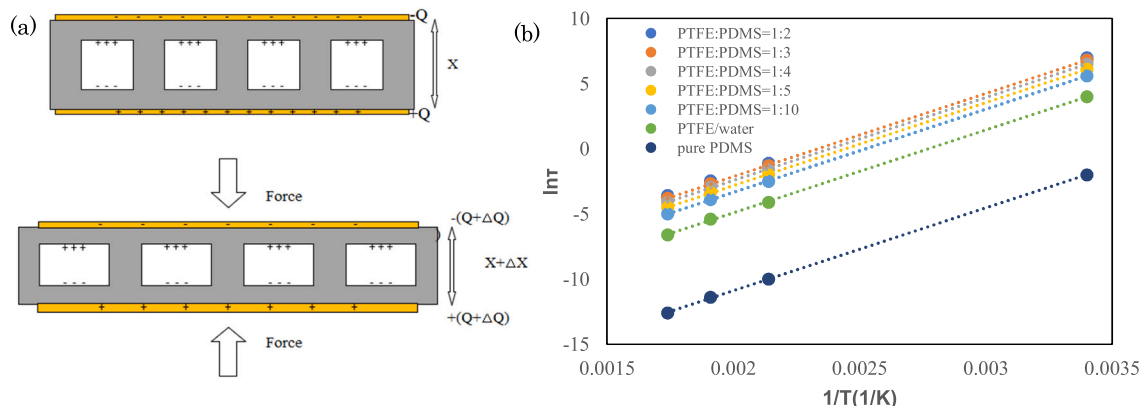


Fig. 1. (a) The working principle of composite layer ferroelectret [4]; (b) The charge decay time-temperature graph of electrets.

water solution is around 55 years ($\ln\tau=4$). In contrast, the storage life of pure PDMS is only one month ($\ln\tau=-2.4$). This demonstrates the ability of the PTFE additive to enhance the charge stability in a PDMS ferroelectret.

It should be noted that in a typical use case scenario, the electret lifetime actually observed is shorter than the predicted value because of the influence of environmental factors such as ambient radiation-induced conductivity and recombination with opposite-polarity ions deposited on the free surface of the samples attracted by the external field effect of the electrets [18].

3. Experimental detail

3.1. Preparation of PDMS ferroelectret and PDMS/PTFE composite ferroelectret

The engineered ferroelectret structure is fabricated using PDMS moulding techniques to realize a contoured PDMS sheet, two of which are subsequently bonded together to form the sealed voids. A Connex 350 TM 3D printer (Stratasys, MN, USA) was used to fabricate the three-dimensional moulds. To prevent the PDMS from sticking to the mould, they were baked in an oven at 80 °C for 24 h and then exposed to a silane vapour for 1 h which results in a thin coating of trichloro (1 H,1 H,2 H,2 H-perfluorooctyl) silane (Sigma Aldrich, MO, USA) [6].

Using the processed moulds, the PDMS ferroelectret can be

fabricated. For the standard pure PDMS ferroelectret, liquid PDMS and curing agent (Sylgard 184 from Dow Corning, MI, USA) were mixed at a 10:1 wt ratio and then degassed in a vacuum desiccator. The prepared degassed PDMS was poured into the moulds and degassed again and then oven baked at 80 °C for 2 h. The thickness of the samples is controlled by the level of the PDMS poured into the mould. After curing, the polymerized PDMS was peeled away from the moulds. The PTFE coatings can be applied to the void surfaces at this point by applying the PTFE layer to the bottom of the contoured structure as described below and shown in Fig. 2. Then an oxygen plasma treatment (Femto Asher, Diener, Germany, 30 S at 35–40 W) was then used to prepare the surfaces of the two PDMS parts and these are bonded together, and oven baked at 80 °C for 1 h. The schematic diagram of the cross-section view of the pure PDMS ferroelectret is shown in Fig. 3(a) and (b).

The PDMS/PTFE composite ferroelectret was fabricated using the approach described above but different ratios of PTFE powder were first added to the PDMS (described in Section 3). Due to the PTFE content, these two parts cannot be bonded by the plasma treatment, so a thin layer of the PDMS/PTFE composite liquid was used as a glue to bond them together. The bonded assembly was then baked in an oven at 80 °C for 1 h. The schematic diagram of the cross-section view of the PDMS/PTFE composite ferroelectret is shown in Fig. 3(c).

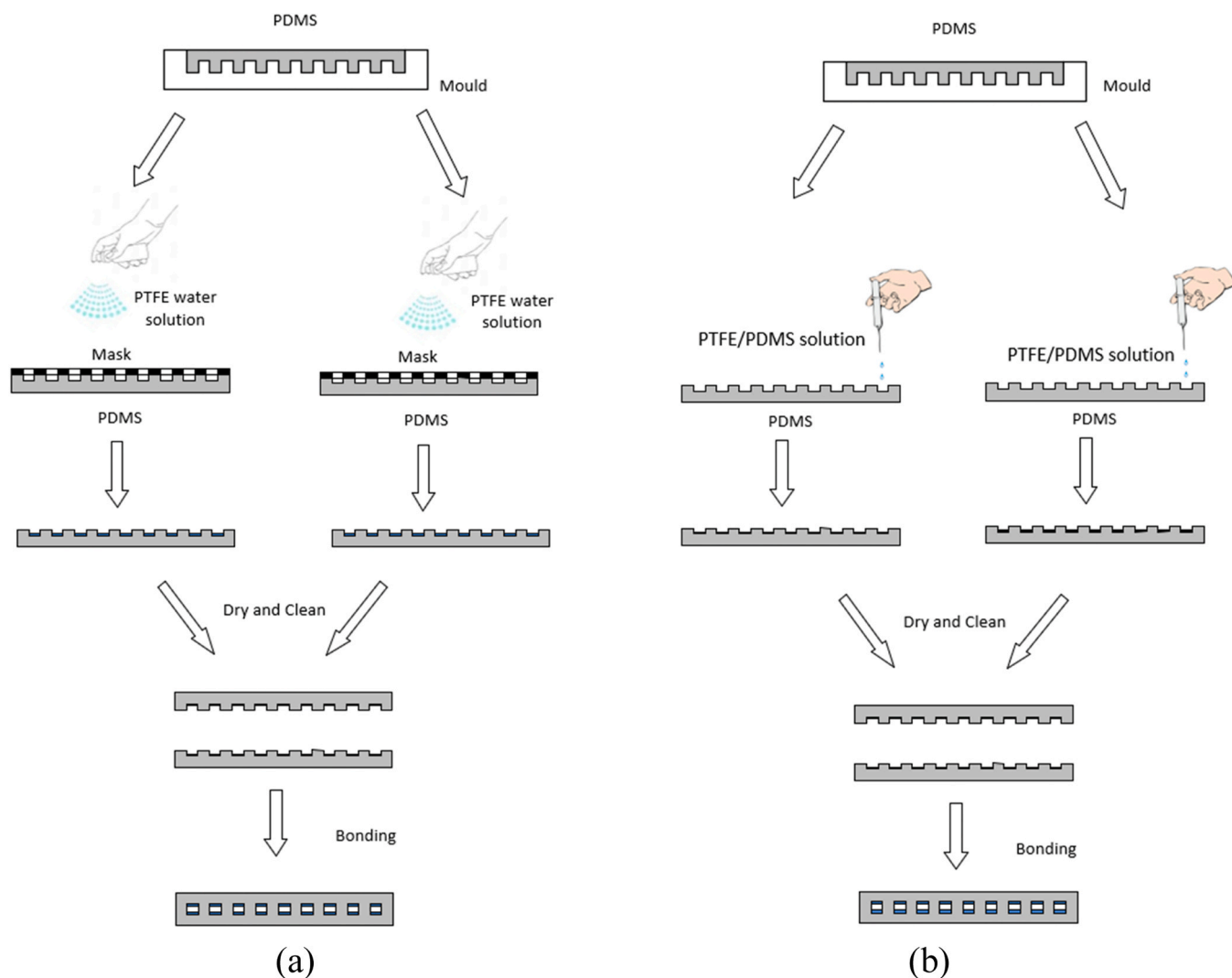


Fig. 2. The fabrication process of two different composite layer ferroelectret (a) PTFE/water solution ferroelectret (b) PDMS/PTFE composite layer ferroelectret.

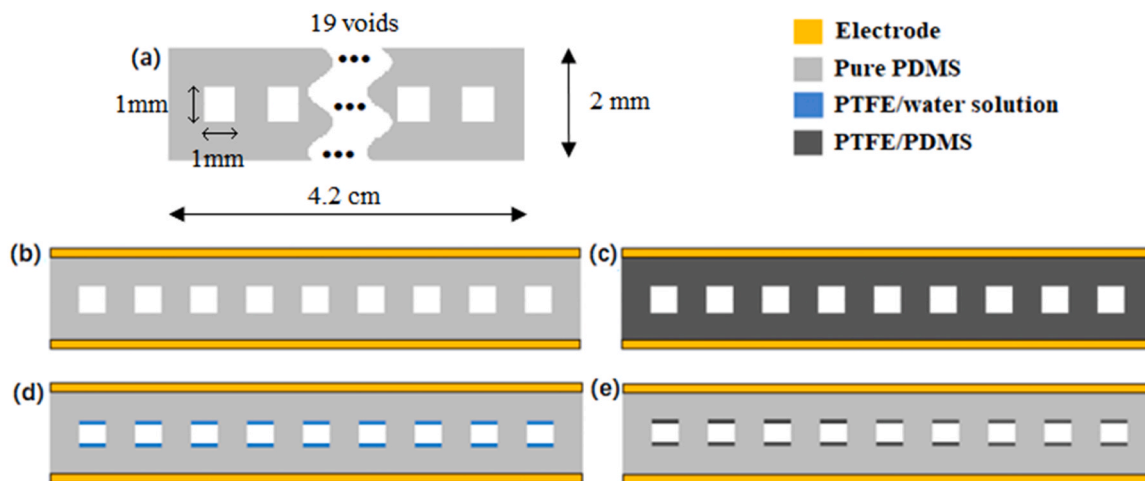


Fig. 3. (a) Dimensions of test sample. Schematic cross-sectional views of (b) pure PDMS ferroelectret; (c) PDMS/PTFE composite ferroelectret; (d) PTFE/water solution ferroelectret; (e) PDMS/PTFE composite layer ferroelectret.

3.2. Preparation of PTFE/water solution layer ferroelectret

The PTFE/water solution was made by mixing 60% by weight of PTFE powder average particle size 1 μm diameter (Sigma Aldrich, MO, USA) to water. The PTFE/water solution was sprayed evenly across the PDMS structure through a stencil mask to pattern the deposition, allowing it to coat the void surface whilst preventing the PTFE solution

from coating the top, bonding surface of the molded PDMS. The samples were then oven baked at 80 $^{\circ}\text{C}$ for 1 h leaving a dried, thin PTFE layer (80 μm) on the void surface. The schematic diagram of the cross-section view of the PTFE/water solution ferroelectret is shown in Fig. 3(d). The fabrication details are shown in Fig. 2(a).

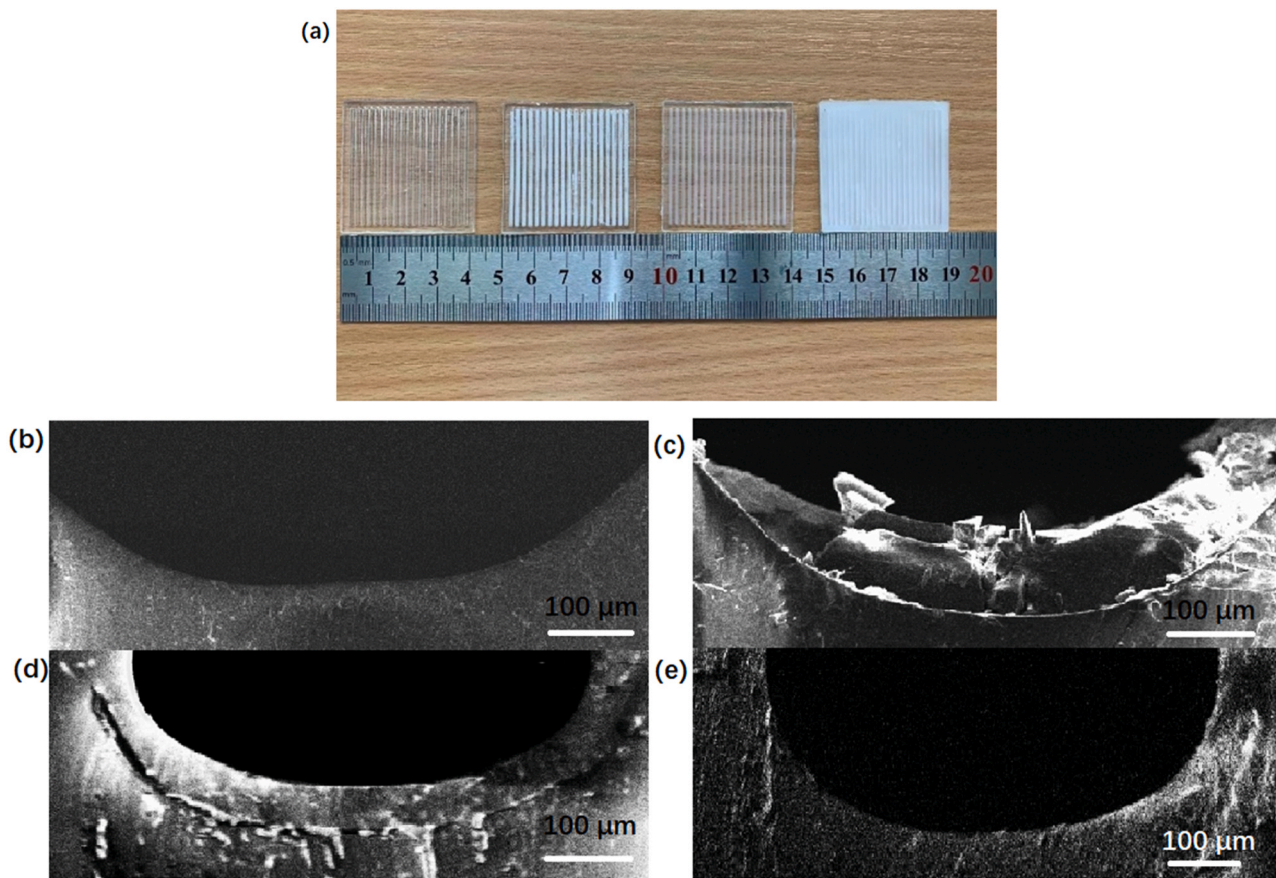


Fig. 4. (a) Photo of samples, from left to right: pure PDMS ferroelectret, the PTFE/water solution ferroelectret, the PDMS/PTFE composite layer ferroelectret, and the PDMS/PTFE composite ferroelectret. (b) SEM photo of the cross-section view of pure PDMS ferroelectret. (c) SEM photo of the cross-section view of PTFE/water solution ferroelectret. (d) SEM photo of the cross-section view of PDMS/PTFE composite layer ferroelectret. (e) SEM photo of a cross-section view of PDMS/PTFE composite ferroelectret.

3.3. Preparation of PDMS/PTFE composite layer ferroelectret

The PDMS/PTFE composite material was made at different ratios of PTFE powder. The powder was mixed evenly with the gelatinous liquid PDMS in weight ratios of 1:10, 1:5, 1:4, 1:3 and 1:2. A syringe was used to manually deposit a fixed dose (0.1 ml) of the liquid solution onto the void surfaces, after which it was allowed to spread across the surface and settle before being baked in an oven at 80 °C for 1 h, as shown in Fig. 4 (b). This leaves an 80 μm PDMS/PTFE composite layer coated in the void surface. The schematic diagram of the cross-section view of the PDMS/PTFE composite layer ferroelectret is presented as Fig. 3(e). For all samples, the external electrode was aluminium tape bonded to the top and bottom surfaces.

3.4. Sample characterization

To explore how the electret properties of the material are affected by the addition of the PTFE, all samples were polarized using identical corona charging parameters which were a charging voltage of 30 kV, charging distance of 4 cm and applied for a time of 2 min. The corona poling process is described in [21]. Since the surface charge density is directly linked to the effective piezoelectric coefficient d_{33e} , the charge decay over time for the 4 samples has been monitored by measuring the effective d_{33e} using a PiezoMeter Systems (PM300, Piezotest Ltd). To evaluate energy harvesting performance, an Instron electrodynamic instrument (ElectroPuls E1000) was used to apply forces to the test samples and the output voltage and voltage across a storage capacitor have been measured.

In order to investigate the durability of these samples, cyclical compressive and bending tests were applied. using The Instron electrodynamic instrument (ElectroPuls E1000) was used to apply a cyclical 500 N compressive force and the change in electrical characteristics of the samples was measured after a predetermined number of compressions. In the bending test, the samples were cyclically deformed around a cylinder with a diameter of 3 cm equating to a bending radius of 1.5 cm with the weight of 1 kg applied to provide tension in the material.

4. Results and discussion

As shown in Figs. 3(a) and 4(a), all the samples were 4.2 cm × 4.2 cm square-shaped with 19 voids inside. The thickness of the samples was 2 mm with a 1 mm void thickness. Fig. 4(b) is the SEM photo of the cross-section view of the pure PDMS ferroelectret. Fig. 4(c) is the SEM photo of the cross-section view of PTFE/water solution ferroelectret. Fig. 4(d) and Fig. 4(e) show the SEM photo of the cross-section view of PDMS/PTFE composite layer ferroelectret and PDMS/PTFE composite ferroelectret where the white dots are the PTFE powders.

The effect of the different weight ratios of PDMS/PTFE on the PDMS/PTFE composite and PDMS/PTFE composite layer ferroelectrets is shown in Fig. 5(a) and (b). As the ratio of PTFE particles increases both the amount of internal surface charge and the mechanical stiffness of the composite PDMS increases. The increase in surface charge is offset by the reduced displacement for a given mechanical force and at ratios beyond 1:3 this leads to a reduced effective d_{33e} . The mechanical

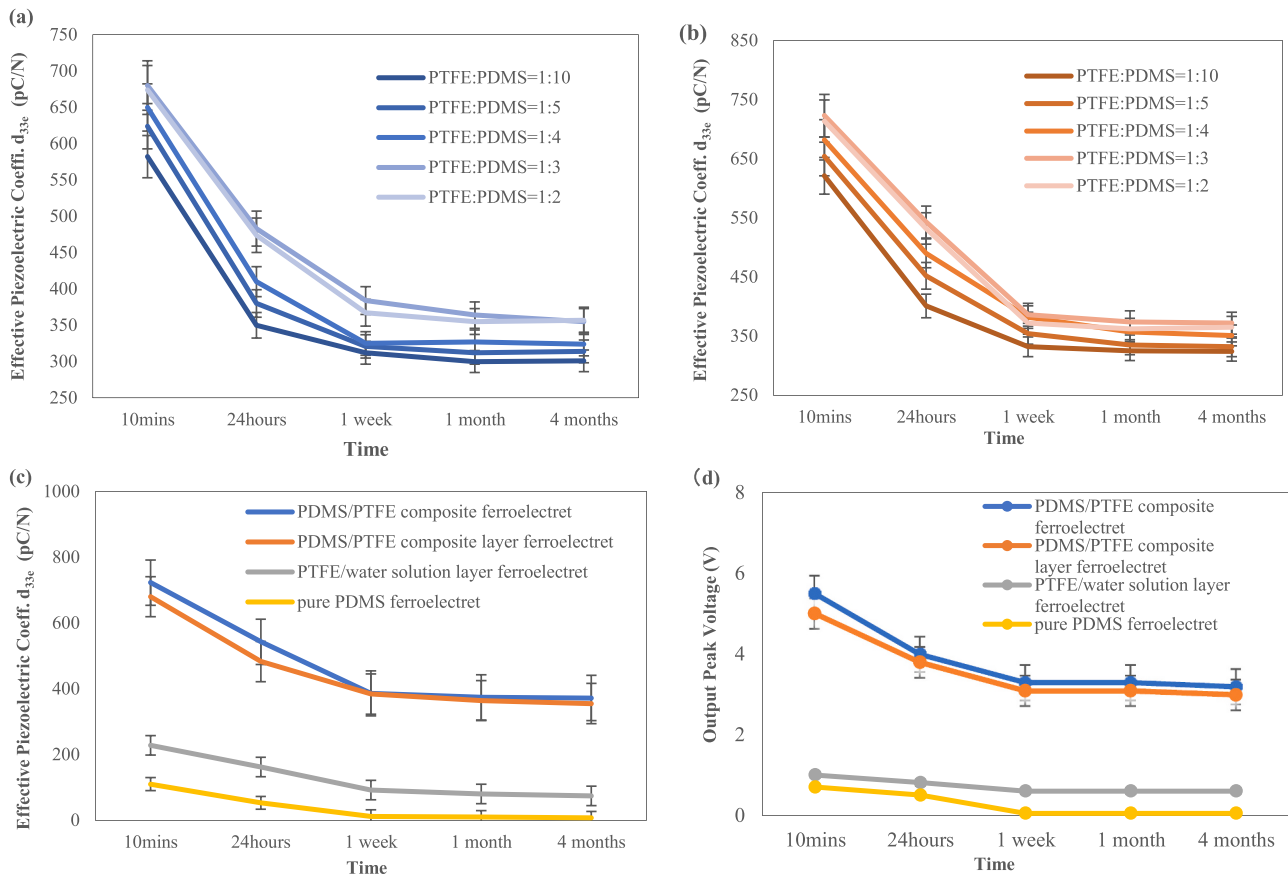


Fig. 5. (a) The piezoelectric coefficient value with different weight ratio of PDMS/PTFE composite ferroelectret (b) The effective piezoelectric coefficient d_{33e} value with different weight ratio of PDMS/PTFE composite layer ferroelectret (c) The effective piezoelectric coefficient d_{33e} value of four different types ferroelectret versus time (the PTFE/PDMS weight ratio of PDMS/PTFE composite ferroelectret and PDMS/PTFE composite layer ferroelectret are 1:3) (d) The output peak voltage versus time under compressive force of 500 N (the PTFE/PDMS weight ratio of PDMS/PTFE composite ferroelectret and PDMS/PTFE composite layer ferroelectret are 1:3).

stiffness of the different materials is presented later.

The corresponding initial effective maximum values of d_{33e} were 723 pC/N and 680 pC/N for the PDMS/PTFE composite and composite layer ferroelectrets respectively. These values are approximately 3 times greater than that of the PTFE/water solution layer ferroelectret (228 pC/N) and 6 times greater than that of the pure PDMS ferroelectret (110 pC/N). Increasing the concentration beyond a ratio of 1:3 does not result in further increases in the effective piezoelectric coefficient d_{33e} .

Fig. 5(c) shows a comparison of the drop in piezoelectric performance over time of the pure PDMS, PTFE solution layer, PDMS/PTFE composite layer and the PDMS/PTFE composite ferroelectrets. The PDMS/PTFE composite layer and PDMS/PTFE composite ferroelectrets maintained around 50% of their initial effective piezoelectric coefficient after 4 months, while the PTFE/water solution ferroelectret only retained around 34%. The effective d_{33e} of the pure PDMS ferroelectret dropped to below 10 pC/N in one month. These results are consistent

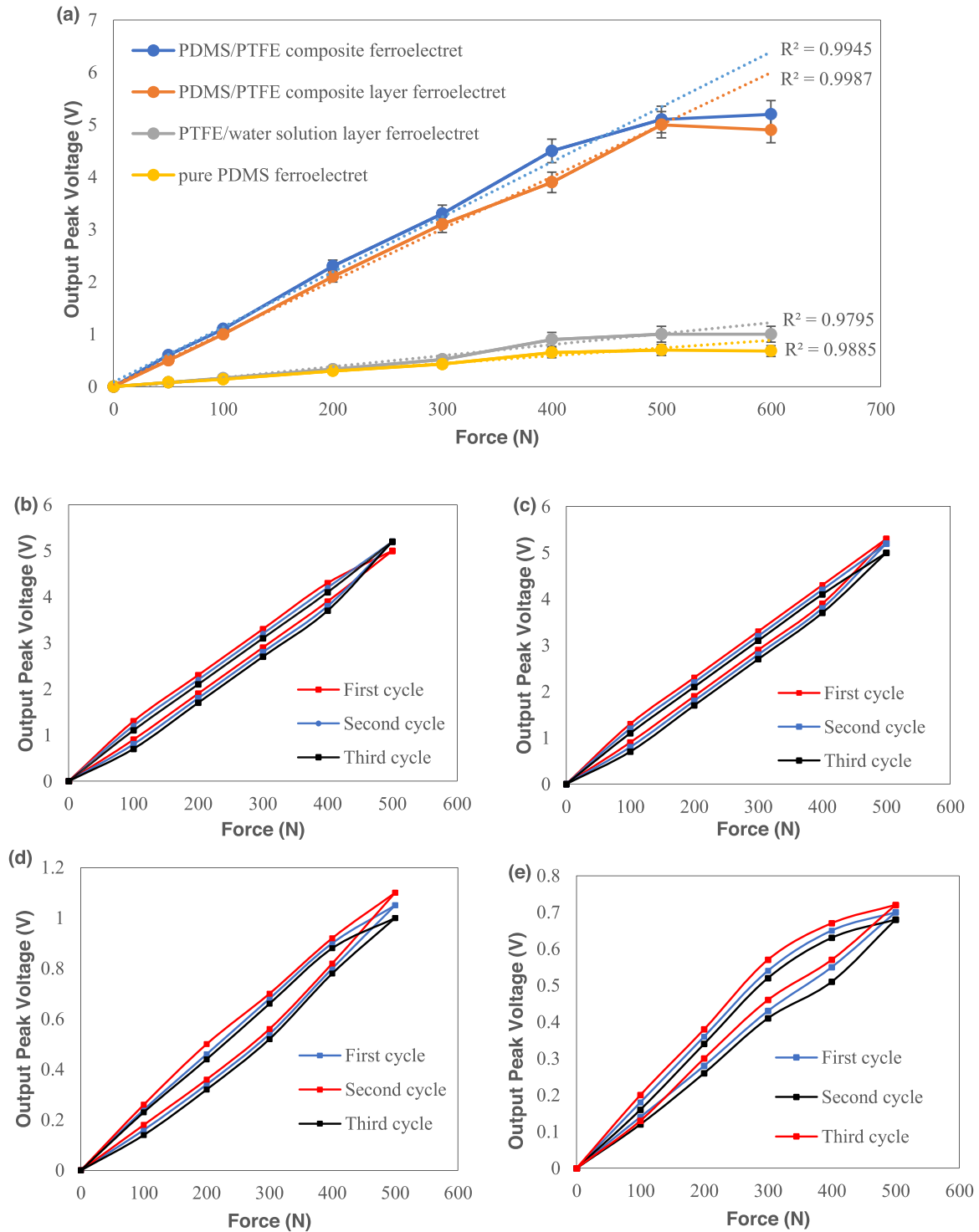


Fig. 6. (a) The output peak voltage by different force at a frequency of 1 Hz and the fitting curve in the linear region by the least square method (b) The hysteresis loop of the PDMS/PTFE composite ferroelectret (c) The hysteresis loop of the PDMS/PTFE composite layer ferroelectret (d) The hysteresis loop of the PTFE/water solution ferroelectret (e) The hysteresis loop of the pure PDMS ferroelectret.

with the predicted charge decay shown in Fig. 1(b).

The variation in the peak output voltage of the four types of ferroelectret under a cyclical compressive force of 500 N (frequency of 1 Hz, averaged from 20 cycles) over time is shown in Fig. 5(d). The maximum peak voltages occurred immediately after corona charging were 5.5, 5, 1 and 0.7 V for the PDMS/PTFE composite (weight ratio 1:3), PDMS/PTFE composite layer (weight ratio 1:3), PTFE/water solution and pure PDMS ferroelectrets respectively. The maximal peak voltage 4 months after corona charging had fallen to 3.3, 3, 0.6 and 0.05 V respectively. The PDMS/PTFE composite and PDMS/PTFE composite layer ferroelectrets retained approximately 60% of their output voltage after 4 months.

The peak output voltage of the four types of ferroelectret under different compressive forces ranging from 0 to 600 N (average taken from 20 cycles applied at a frequency of 1 Hz) is shown in Fig. 6(a). The output peak voltage initially increases with increasing force but levels off at around 500 N at which point the inner voids within the ferroelectret have been fully compressed. The point at which the compression occurs depends upon the fabricated geometries and stiffness of the materials. To explore the sensitivity and linearity of each ferroelectret, the least square method [22] was used to form the straight-line approximations shown in Fig. 6(a) where each point corresponds to measured values. The straight-line approximations were calculated from the data from 0 to 500 N and the sensitivity can be determined by the slope of the dotted straight-line approximations. The values for sensitivity are 10.5, 9.9, 2.1, 1.6 mV/N for the PDMS/PTFE composite ferroelectret, the PDMS/PTFE composite layer ferroelectret, the PTFE/water solution ferroelectret and the pure PDMS ferroelectret respectively.

The linearity can be characterized by R-squared (R^2 , coefficient of determination, a statistical measure for how well date fits linear regression models) or the nonlinearity error. R^2 can be calculated from the straight-line approximations and the closer R^2 is to 1, the better the linearity. Another method involves calculating the nonlinearity error, δ , which can be expressed by Eq. (2) [23],

$$\delta = \frac{\Delta Y_{\max}}{Y} \times 100\% \quad (2)$$

where ΔY_{\max} is the maximum deviation between measuring results and the straight-line approximations and Y is the full scale of the measured results. The nonlinearity error of the PDMS/PTFE composite ferroelectret, the PDMS/PTFE composite layer ferroelectret, the PTFE/water solution ferroelectret and the pure PDMS ferroelectret is 2.7%, 1.7%, 7% and 8% respectively (calculated from results from 0 to 500 N). These results are closely matched to the measure of linearity provided by the R^2 values in Fig. 6(a).

The hysteresis loops of the different ferroelectrets are presented in Figs. 6(b) to 6(e) with results obtained by incrementally increasing and decreasing the applied force by 100 N. The hysteresis error h' can be calculated by Eq. (3),

$$h' = \frac{\Delta h_{\max}}{Y} \times 100\% \quad (3)$$

where Δh_{\max} is the maximum difference between the outputs in the increasing and decreasing directions. The hysteresis error of the PDMS/PTFE composite ferroelectret, the PDMS/PTFE composite layer ferroelectret, the PTFE/water solution ferroelectret and the pure PDMS ferroelectret is 5.2%, 6%, 10% and 12.8% respectively. The difference could be explained by the variations in stiffness and the surface energy of the materials which may affect how the surfaces release as the force is removed. The PDMS/PTFE composite layer ferroelectret and the PDMS/PTFE composite ferroelectrets show a higher sensitivity and linearity and smaller hysteresis error than the PTFE/water solution ferroelectret and the pure PDMS ferroelectret, showing improved potential for use in sensing applications.

The mechanical robustness of the samples and the material fatigue resistance are also important considerations for the device and these were tested in the set-up shown in Fig. 7(a). Fig. 7(b) and (c) show the cross-sectional view of the PTFE/water solution layer ferroelectret before and after 50 compressive cycles. It can be seen that the layer formed by PTFE/water solution was destroyed by the mechanical deformation caused by the compressive forces. In the bending test, the PTFE/water solution layer is also destroyed in the first few cycles.

The effects of the cyclical compressive and bending forces on the output voltages from the samples are shown in Figs. 7(d) and 7(e). In the case of the compressive tests, the PDMS/PTFE composite ferroelectret, PDMS/PTFE composite layer ferroelectret and pure PDMS ferroelectret show no deterioration in output voltage up to 1000 compressive cycles while the PTFE/water solution layer ferroelectret showed a clear drop in the output voltage after only around 10–50 compressive and bending cycles. This is due to the destruction of the PTFE/water layer during the testing process as shown in Fig. 7(b) and (c).

The results of the cyclical bending tests shown in Fig. 7(e) demonstrate no deterioration in output voltage up to 1000 bending cycles for the pure PDMS and PDMS/PTFE composite layer ferroelectrets. The PTFE/water solution layer ferroelectret again failed between 10 and 50 compressive cycles indicating the dried PTFE layer cannot withstand the lateral strains induced by the bending test. One noticeable difference between the bending and compression test results is for the PDMS/PTFE composite ferroelectret which was damaged after 500 cycles. This is because these samples were assembled using the liquid PDMS bonding process and the level of adhesion is not as high as those bonded by the plasma treatment.

Although the piezoelectric performance of PDMS/PTFE composite ferroelectret is better than that of PDMS/PTFE composite layer ferroelectret, the PDMS/PTFE composite layer ferroelectret is more mechanically robust due to the stronger bond strength. The distribution of the PTFE power in the bulk of the PDMS prevents the plasma bonding process which has a negative effect on the assembled sample's resistance to lateral strains.

To explore the practical energy harvesting potential of the ferroelectret samples, the PDMS/PTFE composite ferroelectret with PTFE/PDMS weight ratio of 1:3 (highest piezoelectric performance) was driven by a cyclical mechanical compressive loading of 500 N at 1 Hz for 40 s. The sample was then connected to a 10 μ F capacitor via the power management circuit in shown in Fig. 8(a). The voltage across the capacitor increases to 0.12 V corresponding to a total energy accumulation after 40 cycles of 0.072 μ J. The average energy stored is 1.8 nJ per cycle which corresponds to an average output power of 1.8 nW. The output current, voltage and power versus resistance are shown in Figs. 8(b) and 8(c). Maximum output power occurs at a load resistance of 15 M Ω , with a peak power of 4 μ W.

The power delivered to the load is far less than the energy through the rectifier mainly due to the impedance mismatch between the rectifying circuit and the optimal resistive load. In order to improve this, Fengben *et al.* [24] proposed a universal power management strategy for triboelectric harvesters which possess a similarly high output impedance. With the implemented power management module (PMM), about 85% energy from the triboelectric harvesters can be converted and output as a steady and continuous DC voltage to the load resistance. The PMM improves the stored energy by a factor of 128 times (from 18.5 μ J to 2.37 mJ) when charging a 1 mF capacitor compared with a full bridge rectifier alone [24]. Use of a power management circuit with improved impedance matching will be essential for energy harvesting applications.

In order to characterize the effect of different PTFE concentrations on the stiffness of the PDMS, stress-strain tests were performed on the ferroelectret samples using the Instron E1000 as shown in Fig. 8(d). Considering the anisotropy of the sample structure, it was chosen to apply stress in the same direction as the voids. The results (Fig. 8(e)) show that the pure PDMS and PDMS/PTFE composite layer

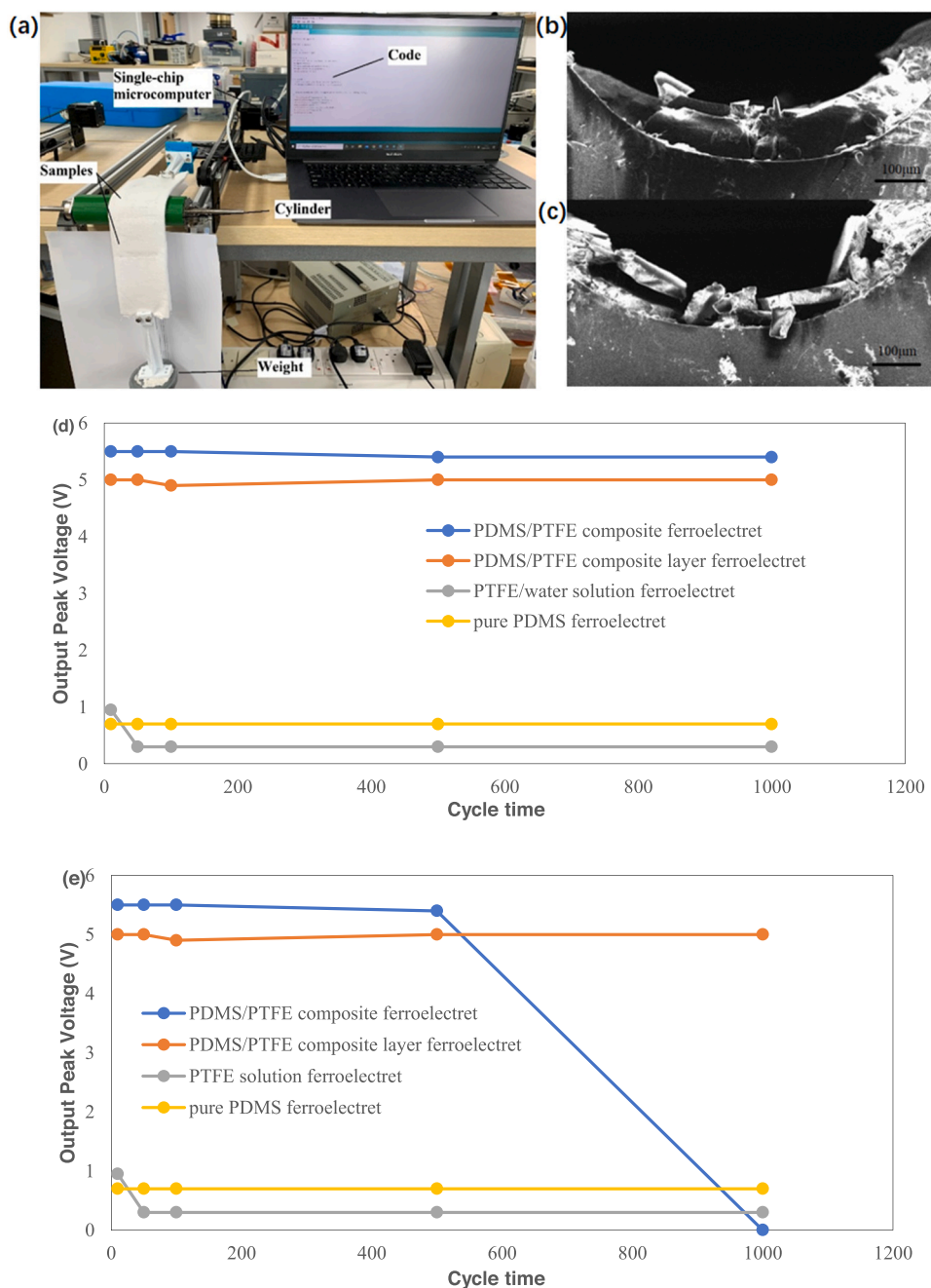


Fig. 7. Mechanical robustness test results. (a) The bending test set-up. (b) Cross-sectional view of PTFE/water solution layer ferroelectret before compression test and (c) after 50 compressive cycles (different sample). (d) Compression test results from different ferroelectret samples under a cyclical compressive force of 500 N applied at a frequency of 1 Hz. (e) The bending test results from different ferroelectret samples.

ferroelectrets have the lowest stiffness and the ferroelectret device can withstand strains of up to 100% without being damaged. The addition of the PTFE particles increases the stiffness of the PDMS and reduces the maximum strain the ferroelectret can withstand. Stiffness increases and the maximum strain decreases with increasing PTFE concentration.

5. Conclusion

This paper illustrates and compares approaches to enhancing the surface charge density and stability in PDMS ferroelectrets. Different approaches to adding the PTFE particles to the ferroelectret structure have been explored and the most obvious approach of simply adding the powder directly to the PDMS to form a composite material for the ferroelectret does produce the most active ferroelectret devices. However,

the addition of the PTFE prevents the device from being assembled using the plasma bonding process. The alternative liquid PDMS bonding process was found to be weaker under lateral strains leading to failure under cyclical bending. Therefore, the application of the PDMS/PTFE composite as a layer within the standard PDMS ferroelectret device was found to be the preferred fabrication approach since it demonstrates significantly improved activity without compromising the robustness of the ferroelectret device. Different concentration ratios of PTFE powder in PDMS were explored and a PTFE/PDMS weight ratio of around 1:3 was found to achieve the highest effective piezoelectric coefficient d_{33e} value of 680 pC/N which is a 6 times improvement compared to the pure PDMS ferroelectret (110 pC/N). Increasing the amount of PTFE beyond this ratio did not provide any further improvement in device output. The PDMS/PTFE composite layer ferroelectret retained 50% of its initial

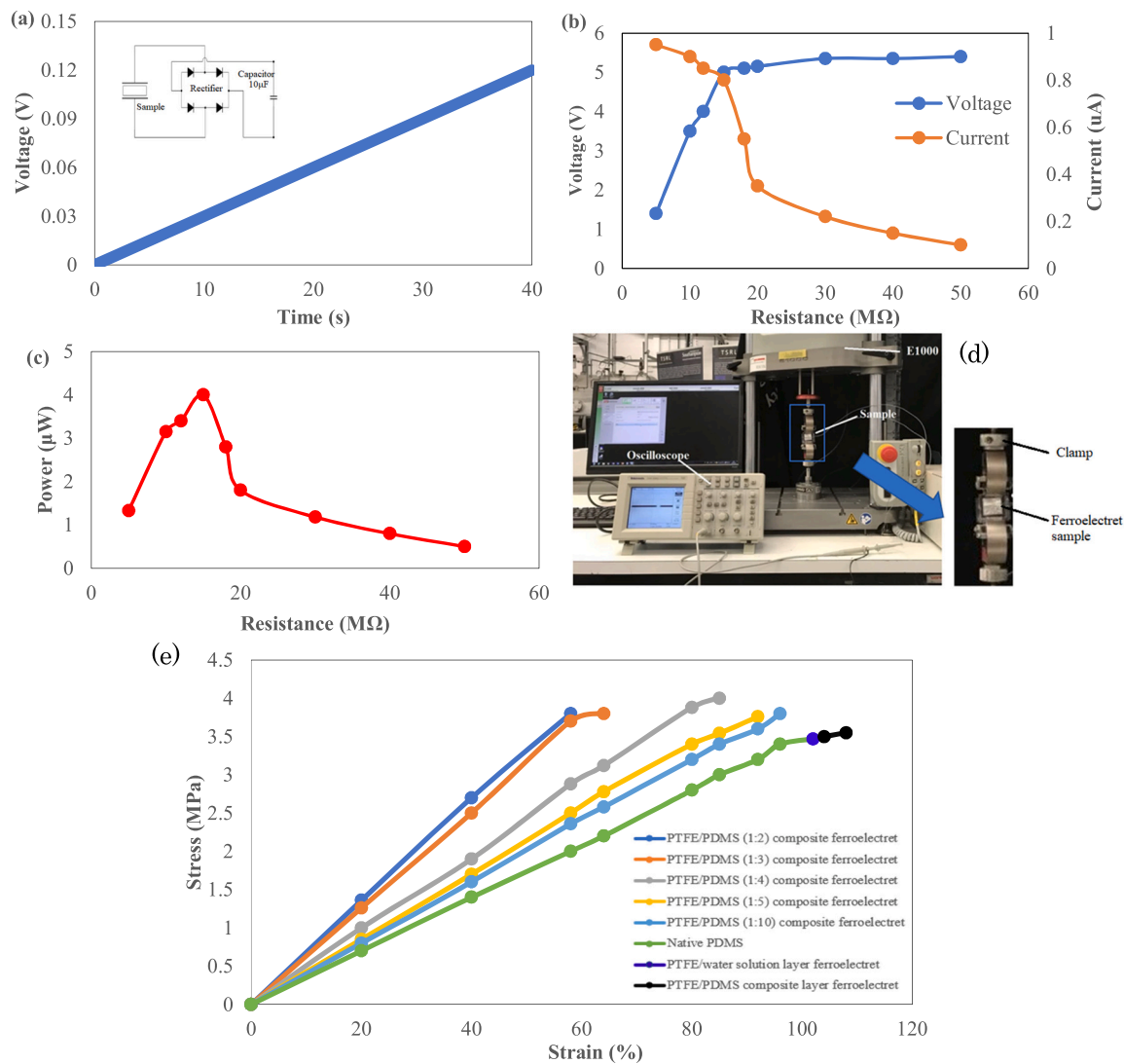


Fig. 8. (a) The power management circuit and the capacitor charging curve up to 40 s (b) Current and Voltage as a function of load resistance. (c) Output power as a function of load resistance. For graphs (a) to (c) a compressive force applied of 500 N was applied at 1 Hz. (d) Stress-strain test set up (Instron E1000). (e) Stress-strain test result for the pure PDMS and composite ferroelectret.

effective piezoelectric coefficient after 4 months again demonstrating a considerable improvement in charge stability compared with the pure PDMS which reduces to less than 10% of the initial, already inferior, effective piezoelectric coefficient value after just one month. Most of the initial charge decay was found to occur in the first week after poling and the composite layer ferroelectret demonstrates excellent stability beyond this point. Adding a layer of pure PTFE using the water-based PTFE solution to the void surfaces was found not to work well due to the mechanically fragile nature of this film. The energy harvesting potential and sensing performance of the PDMS/PTFE composite layer ferroelectret was explored and achieved an output power of 1.8 nW after rectification and a sensitivity of 9.9 mV/N demonstrating its suitability for sensing applications. The soft, compliant and flexible nature of the PDMS material makes it particularly suitable for wearable applications.

Declaration of Competing Interest

The authors declare the following financial interests/personal relationships which may be considered as potential competing interests: Steve Beeby reports financial support was provided by Royal Academy of Engineering.

Data availability

No data was used for the research described in the article.

Acknowledgements

The authors thank the Engineering and Physical Sciences Research Council for supporting this research with grant reference EP/P010164/1. The work of Steve Beeby was supported by the Royal Academy of Engineering under the Chairs in Emerging Technologies Scheme.

References

- [1] P.D. Mitcheson, E.M. Yeatman, G.K. Rao, A.S. Holmes, T.C. Green, Energy harvesting from human and machine motion for wireless electronic devices, *Proc. IEEE* 96 (9) (2008) 1457–1486.
- [2] M.Q. Le, J.F. Capsal, M. Lallart, Y. Hebrard, A. Van Der Ham, N. Reffe, P. J. Cottinet, Review on energy harvesting for structural health monitoring in aeronautical applications, *Prog. Aerosp. Sci.* 79 (2015) 147–157.
- [3] S. Bauer, R. Gerhard-Multhaupt, G.M. Sessler, Ferroelectrets: soft electroactive foams for transducers, *Phys. Today* 57 (2) (2004) 37–44.
- [4] J.J. Wang, T.H. Hsu, C.N. Yeh, J.W. Tsai, Y.C. Su, Piezoelectric polydimethylsiloxane films for MEMS transducers, *J. Micromech. Microeng.* 22 (1) (2011), 015013.

- [5] M. Wegener, S. Bauer, Microstorms in cellular polymers: a route to soft piezoelectric transducer materials with engineered macroscopic dipoles, *ChemPhysChem* 6 (6) (2005) 1014–1025.
- [6] A. Mohebbi, F. Mighri, A. Ajji, D. Rodrigue, Cellular polymer ferroelectret: a review on their development and their piezoelectric properties, *Adv. Polym. Technol.* 37 (2) (2018) 468–483.
- [7] S. Bauer, Piezo-, pyro- and ferroelectrets: soft transducer materials for electromechanical energy conversion, *IEEE Trans. Dielectr. Electr. Insul.* 13 (5) (2006) 953–962.
- [8] J. Zhong, Y. Ma, Y. Song, Q. Zhong, Y. Chu, I. Karakurt, L. Lin, A flexible piezoelectret actuator/sensor patch for mechanical human-machine interfaces, *ACS nano* 13 (6) (2019) 7107–7116.
- [9] A.C. Lopes, C.M. Costa, C.J. Tavares, I.C. Neves, S. Lanceros-Mendez, Nucleation of the electroactive γ phase and enhancement of the optical transparency in low filler content poly(vinylidene)/clay nanocomposites, *J. Phys. Chem. C* 115 (37) (2011) 18076–18082.
- [10] S. Li, A.S. Bhalla, R.E. Newnham, L.E. Cross, Quantitative evaluation of extrinsic contribution to piezoelectric coefficient d_{33} in ferroelectric PZT ceramics, *Mater. Lett.* 17 (1–2) (1993) 21–26.
- [11] Y. Zhang, C.R. Bowen, S.K. Ghosh, D. Mandal, H. Khanbarez, M. Arafa, C. Wan, Ferroelectret materials and devices for energy harvesting applications, *Nano Energy* 57 (2019) 118–140.
- [12] Z. Luo, D. Zhu, J. Shi, S. Beeby, C. Zhang, P. Proynov, B. Stark, Energy harvesting study on single and multilayer ferroelectret foams under compressive force, *IEEE Trans. Dielectr. Electr. Insul.* 22 (3) (2015) 1360–1368.
- [13] Z. Wang, A.A. Volinsky, N.D. Gallant, Crosslinking effect on polydimethylsiloxane elastic modulus measured by custom-built compression instrument, *J. Appl. Polym. Sci.* 131 (22) (2014).
- [14] J. Shi, Z. Luo, Z. Dabin, S. Beeby, Optimization a structure of MEMS based PDMS ferroelectret for human body energy harvesting and sensing, *Smart Mater. Struct.* 28 (7) (2019), 075010.
- [15] Zhang, M., Shi, J., & Beeby, S.P. (2019, December). Improved charge stability in PTFE coatings for PDMS ferroelectrets. In 2019 19th International Conference on Micro and Nanotechnology for Power Generation and Energy Conversion Applications (PowerMEMS) (pp. 1–5). IEEE.
- [16] J. Malecki, A Linear decay of charge in electrets[J], *Phys. Rev. B* 59 (15) (1999) 9954–9960.
- [17] D.K. Davies, Charge generation on dielectric surfaces, *J. Phys. D: Appl. Phys.* 2 (11) (1969) 1533.
- [18] Z. Xia, A. Wedel, R. Danz, Charge storage and its dynamics in porous polytetrafluoroethylene (PTFE) film electrets, *IEEE Trans. Dielectr. Electr. Insul.* 10 (1) (2003) 102–108.
- [19] G.Z. Li, G.G. Wang, D.M. Ye, X.W. Zhang, Z.Q. Lin, H.L. Zhou, F. Li, B.L. Wang, J. C. Han, High-performance transparent and flexible triboelectric nanogenerators based on PDMS-PTFE composite films, *Adv. Electron. Mater.* 5 (4) (2019) 1800846.
- [20] X. Cheng, B. Meng, X. Chen, M. Han, H. Chen, Z. Su, M. Shi, H. Zhang, Single-step fluorocarbon plasma treatment-induced wrinkle structure for high-performance triboelectric nanogenerator, *Small* 12 (2) (2016) 229–236.
- [21] S. Zhukov, S. Fedosov, H. von Seggern, Piezoelectrets from sandwiched porous polytetrafluoroethylene (ePTFE) films: influence of porosity and geometry on charging properties, *J. Phys. D: Appl. Phys.* 44 (10) (2011), 105501.
- [22] H. Abdi, L.J. Williams, Partial least squares methods: partial least squares correlation and partial least square regression. Computational toxicology, Humana Press, Totowa, NJ, 2013, pp. 549–579.
- [23] Y. Huang, S. Zhang, L. Gao, Y. Zheng, Angle measurement technology based on magnetization vector for narrow space applications, *Nanotechnol. Precis. Eng.* 3 (3) (2020) 167–173.
- [24] F. Xi, Y. Pang, W. Li, T. Jiang, L. Zhang, T. Guo, G. Liu, C. Zhang, Z.L. Wang, Universal power management strategy for triboelectric nanogenerator, *Nano Energy* 37 (2017) 168–176.

Mingming Zhang received the MSc degree in Microelectromechanical Systems (MEMS) from University of Southampton. He is currently a full time PhD student in Centre for Flexible Electronics and E-Textiles of the School of Electronic and Computer Science (ECS) at the University of Southampton under supervision of Professor Steve Beeby and Dr. Junjie Shi. He research focuses on the ferroelectret materials and energy-harvesting device.

Dr. Shi received MSc in Microelectromechanical Systems (MEMS) in 2012 and PhD in Electrical and Electronic Engineering in 2017 from University of Southampton, respectively. He is currently a Research Fellow in Centre for Flexible Electronics and E-Textiles of the School of Electronic and Computer Science (ECS) at the University of Southampton. His research interests include energy harvesting from various sources (vibration, wind, human movement, etc.), self-powered systems.

S.P. Beeby obtained his BEng (Hons) in mechanical engineering in 1992 and was awarded his PhD in 1998. He was appointed a Reader in 2008 and was awarded a personal Chair in 2011. He is the RAEng Chair in Emerging Technologies and the director of Centre for Flexible Electronics and E-Textiles, university of Southampton. His research interests include energy harvesting, e-textiles, MEMS, active printed materials development and biometrics. He leads the UK's Energy Harvesting Network and is Chair of the International Steering Committee for the PowerMEMS conference series.